Imaging of the Inner Zone of Blast Furnaces Using Muon Radiography: The BLEMAB Project

S. Gonzi,[1,2] F. Ambrosino,[3,4] P. Andreetto,[5] L. Bonechi,[2] G. Bonomi,[6,7] D. Borselli,[2,8] S. Bottai,[2] T. Buhles,[9] I. Calliari,[10] P. Checchia,[5] U. Chiarotti,[11] C. Cialdai,[2] R. Ciaranfi,[2] L. Cimmino,[3,4] V. Ciulli,[1,2] R. D'Alessandro,[1,2] M. D'Errico,[3,4] F. Finke,[9] A. Franzen,[9] B. Glaser,[12] A. Lorenzon,[5,13] V. Masone,[4] V. Moroli,[11] O. Nechyporuk,[14] L. Pezzato,[10] B. V. Rangavittal,[12] D. Ressegotti,[15] G. Saracino,[3,4] J. Sauerwald,[9] O. Starodubtsev,[2] L. Viliani,[2] and F. Volzone[11]

[1]*Department of Physics and Astronomy, University of Florence, Florence, Italy*

[2]*INFN, Florence Division, Florence, Italy*

[3]*Physics Department "Ettore Pancini", University of Naples "Federico II", Naples, Italy*

[4]*INFN, Naples Division, Naples, Italy*

[5]*INFN, Padua Division, Padua, Italy*

[6]*Department of Mechanical and Industrial Engineering, University of Brescia, Brescia, Italy*

[7]*INFN, Pavia Division, Pavia, Italy*

[8]*Department of Physics and Geology, University of Perugia, Perugia, Italy*

[9]*Ironmaking Department, ArcelorMittal Bremen GmbH, Bremen, Germany*

[10]*Department of Industrial Engineering, University of Padua, Padua, Italy*

[11]*RINA Consulting, Centro Sviluppo Materiali SpA, Rome, Italy*

[12]*Department of Materials Science and Engineering, KTH Royal Institute of Technology, Stockholm, Sweden*

[13]*Department of Physics and Astronomy, University of Padua, Padua, Italy*

[14]*Ironmaking Department, ArcelorMittal Maizières Research SA, Maizières-lès-Metz, France*

[15]*RINA Consulting, Centro Sviluppo Materiali SpA, Dalmine (Bergamo), Italy*

Corresponding author: S. Gonzi
Email: sandro.gonzi@fi.infn.it

Abstract

The aim of the BLEMAB project (BLast furnace stack density Estimation through online Muons ABsorption measurements) is the application of muon radiography techniques, to image a blast furnace's inner zone. In particular, the goal of the study is to characterize the geometry and size of the so-called "cohesive zone", i.e., the spatial region where the slowly downward-moving material begins to soften and melt, which plays such an important role in the performance of the blast furnace itself. Thanks to the high penetration power of natural cosmic-ray muon radiation, muon transmission radiography could be an appropriate non invasive methodology for the imaging of large high-density structures such as a blast furnace, whose linear dimensions can be up to a few tens of meters. A state-of-the-art muon tracking system is currently in development and will be installed at a blast furnace on the ArcelorMittal site in Bremen (Germany), where it will collect data for a period of various months. In this paper, the status of the project and the expectations based on preliminary simulations are presented and briefly discussed.

Keywords: atmospheric muons, imaging, blast furnaces, particle detectors
DOI: 10.31526/JAIS.2022.272

1. INTRODUCTION

Muon radiography is an imaging technique developed within the field of particle and astroparticle physics which, relying on the scattering or on the absorption of muons produced from cosmic-ray interactions in the atmosphere, exploits their capability to penetrate matter. Muon radiography is a noninvasive technique that uses a natural radiation source: thanks to these peculiar characteristics, it has over time been increasingly applied in the investigation of different fields such as archaeology, geology, and civil engineering. Other applications of muon radiography such as those related to geophysics, nuclear waste surveys, homeland security, and natural hazard monitoring have a relevant social impact. This technique allows obtaining three-dimensional or two-dimensional average density distributions of the objects under examination that have thicknesses ranging from a few meters to a few hundred meters. Muon radiography represents thus a powerful tool complementary or alternative to other more common

survey methods, in particular in those cases where the material thicknesses are too large or the volume to be investigated is not accessible.

This paper presents the current status of the BLEMAB (BLast furnace stack density Estimation through online Muons ABsorption measurements) project, the purpose of which is mainly the validation of the muon radiography technology in the steel industry context. This paper is structured as follows. In Section 2, a brief summary of the muon radiography techniques is given. In Section 3, the BLEMAB project is introduced and its technical characteristics are described. In Section 4, and in Section 5 the hardware features and the simulation tools are, respectively, presented and discussed showing some preliminary test results.

2. MUON RADIOGRAPHY

Over the last decades, imaging technology has developed very rapidly, and a variety of techniques have been proposed in various fields of investigation, often characterized by their interdisciplinary nature. Muon radiography, otherwise called "muography", is a widespread and already validated noninvasive technique allowing three-dimensional surveys of volumes having different sizes [1, 2]. The outstanding aspect of this technique is the usage of muons, elementary particles similar to electrons but with a mass about two hundred times larger, as a mean to investigate the internal structure of a target object: the final result, a muon radiography, is the analog of ordinary X-ray radiography. The characteristic that distinguishes it is the ability to probe the interior of large bodies thanks to the greater penetration power of muons compared to X-rays.

Muography is based on the usage of the natural muon flux produced continuously at the upper layers from the interaction of cosmic rays [3] with the nuclei of the atmosphere. During the collision process between primary cosmic rays and the atmospheric nuclei, many secondary particles are usually created and their number starts to increase rapidly as this shower of particles moves downward, toward the Earth. Cosmic showers are mainly composed of pions, protons, electrons, photons, and muons: most of these particles are slowed down and absorbed by the atmosphere, except for muons which have a relatively long lifetime and are highly penetrating, arriving at a rate of roughly $100\,\mathrm{Hz/m^2}$ [3] at sea level. In fact, they constitute the vast majority of the charged particles at sea level (above 1 GeV, the muon flux at sea level is at least two orders of magnitude larger than that of any other charged particle [3, 4]). At sea level, the angular distribution of the atmospheric muon intensity, defined as the flux per unit solid angle, is found to be approximately proportional to $\cos^n\theta$, where θ is the zenith angle and $n \simeq 2$ [5], with a mild dependence of n on energy, latitude, altitude, and depth [6]. This dependence on the zenith angle and on the energy must always be considered given the typical extensions of the objects under examination, especially if they are located in a nearly horizontal direction with respect to the observer.

Two slightly different muography techniques have been developed, adapted to the inspection of volumes of different sizes: multiple scattering muon tomography (MSMT) and muon transmission radiography (MTR).

2.1. Multiple Scattering Muon Tomography (MSMT)

When muons cross materials, their trajectories are continuously modified because of random electromagnetic interactions with the positively charged nuclei: the final effect is a possible nonnegligible overall deflection of the trajectory with respect to the original one. The intensity of this effect, known as "multiple Coulomb scattering", is higher for low-energy particles and increases with the atomic number Z of the traversed medium: this well-known effect is the process behind the multiple scattering muon tomography technique. The instrumentation consists of two independent detectors located upstream and downstream of the target volume: a large set of muon tracks are reconstructed for both detectors and are used to determine the most likely density distribution inside the target volume by means of custom iterative algorithms that are based on the multiple Coulomb scattering effect.

Given the need to reconstruct the muon trajectory before and after the object, the MSMT technique is usually exploited for relatively small objects with linear dimensions of at the most a few meters and provides three-dimensional information on the observed volume.

The MSMT technique has been proposed in 2003 [7] and has subsequently been applied in various fields, ranging from security and environmental protection to homeland security, proving to be usable to detect heavy metals in transport containers, to contrast nuclear contraband, or to detect the shielded radioactive "orphan" sources used, for instance, in manufacturing operations or in hospital equipment [8]. Some interesting industrial applications concerning the imaging of a blast furnace have also been presented in the last decade [9, 10, 11, 12, 13, 14].

2.2. Muon Transmission Radiography (MTR)

Depending on the thickness of the traversed object, a certain number of muons will also be absorbed. The muon transmission radiography technique is based on that consequent reduction of the muon flux intensity. The instrumentation in this case only consists of a single muon telescope that is used to compare the muon flux downstream of a target volume with the muon flux measured in the same direction but in the absence of any target, the so-called free-sky flux.

The MTR technique is usually exploited for relatively large objects, such as mountains and volcanoes, and provides a two-dimensional angular density profile of the target volume, i.e., an estimate of the average density of matter encountered along a given direction within the field of view of the instrument. By repeating the measurement from different angles, a three-dimensional distribution can be eventually derived. By using some custom algorithms, it is also possible to identify some "anomalies" in the two-dimensional angular density profile that could potentially be linked to unexpected cavities or dense objects located somewhere along the identified directions.

The MTR technique has been proposed in 1955 to determine the rock overburden on a mountain tunnel [15]. In 1970, a team led by L. W. Alvarez disproved, with an application of the technique, the possible existence of a hidden burial chamber in Chefren's Pyramid [16]. Following these pioneering measurements, the MTR technique has widely been used for numerous applications in the fields of volcanology, archaeology, and mining ([17, 18, 19, 20], to name a few).

3. THE BLEMAB PROJECT

The main aim of the BLEMAB project is to test the capabilities of the muon transmission radiography technique in the steel industry context. The final goal is to perform the imaging of the internal volume of blast furnaces and to establish a noninvasive investigation methodology for online monitoring of internal density variations of such structures.

A blast furnace is a kind of furnace used in the metallurgical industry to produce metals for further industrial usage, generally pig iron for subsequent processing into steel, but also others such as lead or copper. In a blast furnace, fuel (coke), ores, and flux (limestone) are continuously fed through the top of the furnace, while a hot blast of air (sometimes with oxygen enrichment) is blown into the lower section of the furnace through a series of pipes called "tuyeres" so that the chemical reactions take place throughout the furnace as the material falls downward: the term "blast" refers precisely to the fact that the combustion air is supplied above atmospheric pressure. The end products are usually molten metal and slag phases tapped from the bottom and waste gases exiting from the top of the furnace.

An important region inside a blast furnace is the so-called "cohesive zone", the place in which the softening and melting of the iron ore proceed. The cohesive zone is usually located in the middle part of the furnace, from the lower part of the shaft down to the tuyeres. In many blast furnaces, it is common practice to use the shape and position of the cohesive zone as a control guide for burden distribution. An accurate estimation of the shape and location of the cohesive zone would help steel companies to have better control over the blast furnace process and improve its thermal efficiency and then its productivity.

Until now, this kind of study has been based on a combined approach, using mathematical estimation models and direct measurements realized with probes, in order to have continuous monitoring of the cohesive zone. Different methods have been developed in the past for the direct measurements with probes: the tracking of radioisotopes injected from the top of the blast furnace, the use of vertical probes with conductive cables connected to conventional instrumentation, such as a multipoint vertical probe (MPVP) [21, 22], or other very expensive and invasive techniques, such as core drilling and blast furnace dissection [23]. Unlike these techniques, muon imaging is proposed as a safe noninvasive radiographic methodology based on a completely natural and freely usable radiation, overcoming any radiological safety procedure.

Muon imaging has been proposed in the past for blast furnace imaging [24, 12], showing the feasibility of measuring the density distribution of the lower part of a blast furnace using the muon radiography technique. In particular, the European Mu-Blast project [14] has demonstrated that muons can be used to produce images of the blast furnace interior using both MSMT and MTR techniques. In detail, the MSMT technique requires quite large and heavy detectors, which could pose problems of compatibility with existing blast furnace infrastructures and would be difficult to move to explore different zones: this technique would produce 3D maps of the material density in the central part of the blast furnace showing the position in space, the shape, and the density of material structures inside it. MTR technique instead needs smaller, simpler, and lower cost detectors but can produce only 2D projections of the stopping power of the crossed blast furnace section: placing two or three such small detectors around the blast furnace could give a partial insight into the 3D characteristics of the internal structures with a collection data time that can be of the order of a few hours (compatible with expected density and melting zone changes).

The main goal of the BLEMAB project is a direct measurement of the height of the casting surface by using the MTR technique, with a muon tracking system of large acceptance and appropriate angular resolution suitably developed for the purpose. This equipment will be installed at the blast furnaces hosted in the ArcelorMittal site in Bremen (Germany) [25] for many months, in order to allow long-term data collection and the development of a monitoring methodology based on the online analysis of muon trajectories and on the comparison with realistic simulations. Muographic measurements will also be compared with measurements obtained using an enhanced multipoint vertical probe (E-MPVP) and standard blast furnace models for validation.

3.1. Imaging Methods with the MTR Technique

The aim of the MTR technique is the measurement of the transmission, defined as the ratio (as a function of the zenith and azimuth angles, θ and φ) between muon fluxes upstream and downstream of the target object. Measurements are performed by using charged-particle trackers that are able to determine the angles defining the detected muon arrival direction by reconstructing in space its trajectory. The upstream flux is not directly accessible for large targets as it would be impractical to place a sufficiently large detector on top, so a "free-sky measurement" is performed instead by pointing the detector in the same direction but without the target in its field of view. As the experimental apparatus and its operating conditions are the same for the two measurements, most factors (such as the sensitive area of the muon tracker, its angular acceptance, and the trigger efficiency) cancel in the ratio. By assuming as a further simplification that the detector dead time is negligible with respect to the total acquisition time, the measured muon transmission T^{M} will be given by the formula

$$T^{\mathrm{M}}(\theta,\varphi) = \frac{N_{\mathrm{T}}(\theta,\varphi)}{N_{\mathrm{FS}}(\theta,\varphi)} \cdot \frac{t_{\mathrm{FS}}}{t_{\mathrm{T}}} \tag{1}$$

where $N_{\mathrm{T}}(\theta,\varphi)$ and $N_{\mathrm{FS}}(\theta,\varphi)$ are the angular distributions of muon reconstructed tracks measured, respectively, downstream from the target (T) and looking at the free-sky (FS) in the respective data acquisition time t_{T} and t_{FS}.

To extract information on the density distribution inside the target volume, a comparison with a muon transmission obtained from simulation T^S is required. Simulations need to take into account a realistic muon flux describing the angular and energy spectra at ground level, the detailed external geometry of the volume under examination, and an estimated average value of the volume density. The comparison of the measured two-dimensional angular distribution of muon transmission with realistic software simulations allows reconstructing the two-dimensional average angular density distribution of the target, as resulting from the measuring position. Combining multiple measurements performed from different view angles, information on the three-dimensional density distribution can be derived.

4. EXPERIMENTAL APPARATUS

The application of the muon transmission radiography survey method for the BLEMAB project requires the installation of a muon tracking system downstream of the blast furnace volume. Two independent muon trackers will be realized in such a way to have the possibility of installing them both in the same blast furnace, in order to have a stereoscopic view of the structure, or in two different blast furnaces at the same time, in order to perform a comparative study of different structures.

Each of these trackers will be made of three independent $(80 \times 80)\,\mathrm{cm}^2$ surface modules, based on the same technology used for the MURAVES [26] and MIMA [27] projects, which will measure two coordinates of muon impact points along two orthogonal axes (XY). Each XY tracking module will be composed of two stacked tracking planes, each of which consists of 64 scintillator bars, with a triangular-based prism shape having a dimension at the base of 25 mm and a length of 800 mm. The orientation of the bars in the two planes will be orthogonal to each other. The scintillator material chosen for the BLEMAB detectors is a good quality fast organic polystyrene-based plastic. Each scintillator bar will be read by means of silicon photomultipliers (SiPM) optical sensors having an optimized quantum efficiency in correspondence with the emission spectrum of the selected scintillator. Each tracking module will be read out by means of four custom data acquisition (DAQ) slave boards housing a 32-channel front-end extended analog SiPM integrated readout chip (EASIROC1B) [28] and an application-specific integrated circuit (ASIC) to control the front-end circuitry and the transmission of data to a central custom DAQ master board implementing the trigger logic and data collection from up to 16 slave boards. A Raspberry PI [29] miniaturized computer, connected to the master DAQ board, will be used to set up the whole electronic chain, receive the data packet from the master DAQ board, and write it to physical support. A network access to the detector will be available at the ArcelorMittal blast furnace in order to allow online detector control and synchronization of data to a remote server. A single muon tracker, an assembly of three XY tracking modules, will be enclosed in a light aluminum box and mounted on an altazimuth platform, which will allow modifying the telescope pointing direction. The whole measuring system will be housed inside a large metal frame, completely covered by metal panels, to protect the apparatus from possible blows, splashes of liquids, and corrosive vapors. Because the environment of a blast furnace is usually characterized by quite high temperatures, a cooling system based on a water chiller will be housed inside the same protection frame and the cooling line will be put in contact with the box housing the detector, in order to protect the optical sensors.

4.1. Test on a Prototype Tracking Plane

A first partial prototype of a tracking plane has been produced in order to estimate the detection efficiency that is possible to obtain in the BLEMAB detector configuration. This prototype is made of five scintillator bars enclosed in a protective aluminum box used also as a darkening cover. Each bar has been read out by two SiPM optical sensors whose signals have been summed together.

A study of the dependence of detection efficiency on the impact coordinate of muons along the bars has been carried out by using an external trigger system made of two auxiliary plastic scintillators read by means of standard photomultiplier tubes (PMTs): these scintillators have a small surface and are suitable to select a small region of the system under test. The complete setup used for the test is reported in Figure 1(a). Data taking was repeated for seven different positions of the trigger system, with steps of 10 cm, in order to cover the whole length of the prototype, corresponding to 80 cm. For each position, a total of approximately 1,000 muon events have been collected, and the signals have been treated with a custom DAQ system (a Teledyne LeCroy HDO6054 digital oscilloscope [30]). Figure 1(b) shows the variation of the detection efficiency for the different impact point positions: the values are all compatible with a constant value of 99.7% within the statistical uncertainties. All measured values are anyway above 99.6%.

5. SOFTWARE SIMULATIONS

Software simulations are required initially to provide preliminary estimates of the expected muon rate, in order to define the minimum size of the apparatus allowing a statistically relevant measurement in the required time. Software simulations are also required to perform comparisons with real measurements, allowing converting the two-dimensional muon transmission maps in average density maps.

5.1. Fast Simulation Tool

A preliminary simulation has been carried out with a fast and simplified custom tool that has successfully been used by the team involved in the BLEMAB project for many applications of the MTR technique in the field of geology [31, 32, 33], archaeology [34], and civil engineering [35]. This simulation tool requires the knowledge of the material thickness $l(\theta, \varphi)$ seen from the detector's installation position along each direction defined by the zenith and azimuth angles and the estimated average density ρ of the

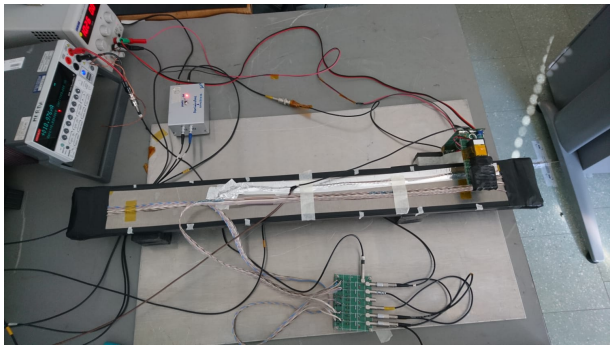

(a) Complete setup used for the test

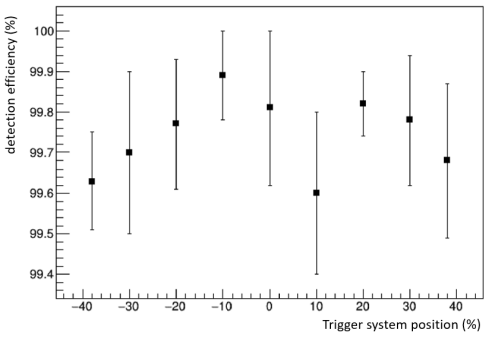

(b) Detection efficiency as a function of the muon impact point coordinate

FIGURE 1: Setup and results of a detection efficiency test performed on a tracking module prototype. The coordinate axis is oriented parallel to the scintillator bars.

traversed medium. The product of these two quantities determine the material opacity along each direction

$$X(\theta, \varphi, \rho) = \rho \cdot l(\theta, \varphi). \tag{2}$$

The following step is to compute the simulated muon integral flux Φ^{S} in a target and free-sky configuration

$$\begin{aligned} \Phi^{S}_{T}(\theta, \varphi, \rho) &= \int_{E_{min}(X)}^{\infty} \phi(\theta, \varphi, E) dE, \\ \Phi^{S}_{FS}(\theta, \varphi) &= \int_{E_0}^{\infty} \phi(\theta, \varphi, E) dE, \end{aligned} \tag{3}$$

where $\phi(\theta, \varphi, E)$ is the differential muon flux as a function of both the muon incoming direction (θ, φ) and muon energy E, $E_{min}(X)$ is the minimum energy that muons must have in order to cross the opacity X and reach the detector in the target configuration, E_0 is the minimum energy required to detect muons in the free-sky configuration because of the opacity of the detector itself. The minimum muon energy $E_{min}(X)$ was obtained from the opacity X by using the tabulated values present in the literature [36]. For the differential muon flux $\phi(\theta, \varphi, E)$, we used the one measured by the ADAMO experiment [37]. The ADAMO measurements were performed in Florence at various angles from the vertical to almost the horizontal direction ($\theta_{max} = 80°$), and they turned out to be consistent with other measurements in the literature in the high energy range, while they slightly differ in the low energy range because of solar modulation. The corresponding simulated muon transmission $T^{S}(\theta, \varphi, \rho)$ is finally calculated as

$$T^{S}(\theta, \varphi, \rho) = \frac{\Phi^{S}_{T}(\theta, \varphi, \rho)}{\Phi^{S}_{FS}(\theta, \varphi)}. \tag{4}$$

In the fast simulation tool the muon tracker is simplified to a point-like detector and the radiation-matter interaction between muons and detector is also not simulated.

Figure 2(a) shows an accurate representation of the ArcelorMittal blast furnaces located in the Bremen site: for each component, a precise geometry in a computer-aided design (CAD) format and a rough estimation of the average density has been provided by the company. A preliminary simulation has been carried out, by means of the fast simulation tool, by placing a point-like detector 8 m far from the wall of the blast furnace. With this setup, a simulated transmission map has been computed in a 1° bin size for both elevation α (the complementary of the zenith angle θ) and azimuth angle φ. Considering the simulated transmission as a hypothetical measured transmission $T^{M}(\theta, \varphi)$, a daily angular distribution of muon events $N_T(\theta, \varphi)$ has been estimated for a MIMA-like detector (the operating detector closest to the chosen design for the BLEMAB project) placed with its centre in the same position of the simulated point-like detector and tilted 45° by inverting the formula (1) and obtaining

$$N_T(\theta, \varphi) = T^{M}(\theta, \varphi) \cdot N_{FS}(\theta, \varphi) \cdot \frac{t_T}{t_{FS}}, \tag{5}$$

where $N_{FS}(\theta, \varphi)$ is the angular distribution of muon events in a free-sky configuration measured by the MIMA experiment in a time t_{FS} equal to 15 days in the same expected experimental conditions and the time t_T is 24 hours. The results of the simulation are shown in Figure 2(b): the presence of the blast furnace in front of the muon detection system can be identified as an elongated angular region in the central part of the distribution, where the number of detected muons is significantly suppressed. A range from about 10 to 70 muon traces are expected in each involved bin after a data collection of about 24 hours, thus allowing the reconstruction of the average directional density with a statistical uncertainty of less than 30%.

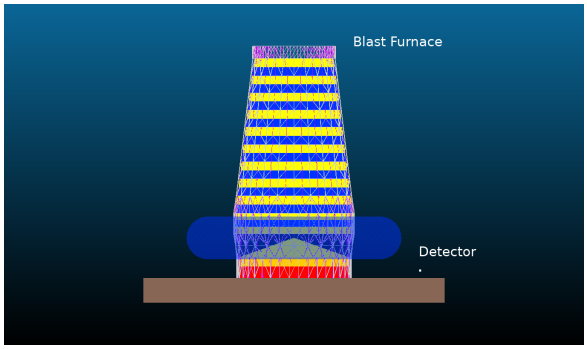

(a) Geometric configuration implemented for the simulation

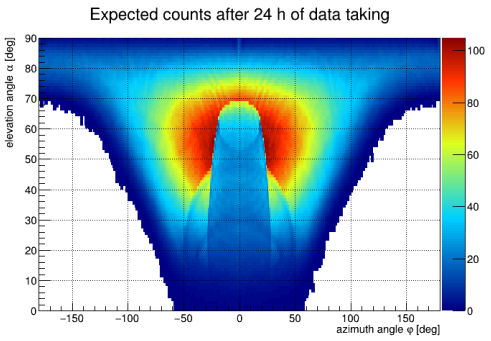

(b) Angular distribution of muon events expected after 24 hours of data taking

FIGURE 2: Setup and results of the simulation performed with the fast simulation tool, where the detector is assumed to be point-like.

5.2. Complete Simulation Tool

A more detailed simulation based on the GEANT4 [38] software package and on the recently released atmospheric muon software generator ECOMUG [39] is currently under development. The basic structure of this simulation was derived from the one created previously within the European Mu-Blast project. In this simulation tool, it is possible to replicate some identical detectors and place them all around the blast furnace at a given radius to the center. The multiple detection systems allow maximizing the ratio between the number of events entering the detector's acceptance and the total number of simulated muon events.

6. CONCLUSIONS

The work reported in this paper describes the status of the European BLEMAB project, a muon imaging application in the steel industry field. In this project, the noninvasive muon transmission radiography technique will be exploited to monitor processes happening inside blast furnaces, with the main purpose of providing information about the effects on the distribution of materials and densities inside the blast furnace itself, when changing the blast furnace's running parameters. A dedicated muon detection system suitable for the installation in such an inhospitable environment is under construction, and a preliminary test on a prototype tracking plane has been produced in order to estimate the detection efficiency that is possible to obtain in the BLEMAB configuration. Software simulation tools are also under development, and a preliminary simulation performed with a simplified and fast tool has shown that the muon transmission radiography technique is able to imagine the blast furnace in the required time of 24 hours. The apparatus will be installed at the ArcelorMittal site in Bremen (Germany) in 2022 for measurement of several months. Muon imaging results will be compared with results obtained with an enhanced multipoint vertical probe and standard blast furnace models describing the variations of internal parameters along the height of the structure, in order to validate the technique and to improve the steel production efficiency.

CONFLICTS OF INTEREST

The authors declare that there are no conflicts of interest regarding the publication of this paper.

ACKNOWLEDGMENTS

This project has received funding from the European Union's Research Funds for Coal and Steel 2019 Programme under grant agreement no. 899263.

References

[1] L. Bonechi et al., Atmospheric muons as an imaging tool, Rev. Phys. **5** (2020), 100038. *DOI: 10.1016/j.revip.2020.100038*.
[2] G. Bonomi et al., Applications of cosmic-ray muons, Prog. Part. Nucl. Phys. **112** (2020), 103768. *DOI: 10.1016/j.ppnp.2020.103768*.
[3] P. A. Zyla et al. (Particle Data Group), Review of Particle Physics, PTEP **2020** (2020) no. 8, 083C01. *DOI: 10.1093/ptep/ptaa104*.
[4] R. L. Golden et al., Measurement of the energy spectra of cosmic ray electron component and protons at ground level, J. Geophys. Res. **100** (1995) no. A12, 23515. *DOI: 10.1029/95JA02449*.
[5] J. W. Lin et al., Measurement of angular distribution of cosmic-ray muon fluence rate, Nucl. Instrum. Meth. A **619** (2010), 24–27. *DOI: 10.1016/j.nima.2009.12.017*.
[6] P. K. F. Grieder, Cosmic rays at earth: Researcher's reference, manual and data book, Elsevier, ISBN 978-0-444-50710-5 (2001).
[7] K. Borozdin et al., Radiographic imaging with cosmic-ray muons, Nature **422** (2003), 277. *DOI: 10.1038/422277a*.

[8] W. C. Priedhorsky et al., Detection of high-Z objects using multiple scattering of cosmic ray muons, Review of Scientific Instruments 74 (2003), 4294–4297. *DOI: 10.1063/1.1606536*.

[9] W. B. Gilboy et al., Industrial thickness gauging with cosmic-ray muons, Radiation Physics and Chemistry **74** (2005) no. 6, 454–458. *DOI: 10.1016/j.radphyschem.2005.08.007*.

[10] K. Nagamine et al., Probing the inner structure of blast furnaces by cosmic-ray muon radiography, Proceedings of the Japan Academy, Series B **81** (2005) no. 7, 257–260. *DOI: 10.2183/pjab.81.257*.

[11] J. Sauerwald et al., Investigation of the coke network and cohesive zone by muon tomography, Stahl und Eisen **134** (2014), 29–38.

[12] E. Åström et al., Precision measurements of Linear Scattering Density using Muon Tomography, JINST **11** (2016) no. 07, P07010. *DOI: 10.1088/1748-0221/11/07/P07010 [arXiv:1605.07605 [physics.ins-det]].*

[13] X. Hu et al., Exploring the capability of muon scattering tomography for imaging the components in the blast furnace, ISIJ Int. **58** (2018) no. 1, 35–42. *DOI: 10.2355/isijinternational.ISIJINT-2017-384*.

[14] P. Zanuttigh et al., Study of the capability of muon tomography to map the material composition inside a blast furnace (Mu-Blast) - Final report, Publications Office of the European Union, ISSN 1831–9424 (2019). *DOI: 10.2777/24858*.

[15] E. P. George, Cosmic rays measure overburden of tunnel, Commonwealth Engineer, July 1 (1955) 455–457.

[16] L. W. Alvarez et al., Search for hidden chambers in the pyramids, Science **167** (1970), 832–839. *DOI: 10.1126/science.167.3919.832*.

[17] H. Tanaka et al., Development of a two-fold segmented detection system for near horizontally cosmic-ray muons to probe the internal structure of a volcano, Nucl. Instrum. Meth. A **507** (2003) no. 3, 657–669. *DOI: 10.1016/S0168-9002(03)01372-X*.

[18] F. Ambrosino et al., The MU-RAY project: detector technology and first data from Mt. Vesuvius, JINST **9** (2014), C02029. *DOI: 10.1088/1748-0221/9/02/C02029*.

[19] K. Morishima et al., Discovery of a big void in Khufu's Pyramid by observation of cosmic-ray muons, Nature **552** (2017) no. 7685, 386–390. *DOI: 10.1038/nature24647 [arXiv:1711.01576 [physics.ins-det]].*

[20] E. Guardincerri et al., 3D Cosmic Ray Muon Tomography from an Underground Tunnel, Pure Appl. Geophys. **174**, (2017), 2133–2141. *DOI: 10.1007/s00024-017-1526-x*.

[21] S. Zaimi et al., Blast Furnace models development and application in ArcelorMittal Group, Rev. Met. Paris **106** (2009) no. 3, 105–111. *DOI: 10.1051/metal/2009021*.

[22] S. J. van der Stel et al., Stable blast furnace control by advanced measurement technique, presentation at METEC 2015 conference (15–19 June 2015, Düsseldorf, Germany).

[23] K. Kanbara et al., Dissection of Blast Furnaces and Their Inside State, Tetsu-to-Hagane **62** (1976) no. 5, 535–546. *DOI: 10.2355/tetsutohagane1955.62.5_535*.

[24] A. Shinotake et al., Probing the inner structure of blast furnace by cosmic ray muon radiography, Tetsu-to-Hagane **95** (2009) no. 10, 665–671. *DOI: 10.2355/tetsutohagane.95.665*.

[25] ArcelorMittal Bremen GmbH, ArcelorMittal Bremen (website). https://bremen.arcelormittal.com Accessed January 10, 2022.

[26] M. D'Errico et al., Muon radiography applied to volcanoes imaging: the MURAVES experiment at Mt. Vesuvius, JINST **15** (2020) no. 03, C03014. *DOI: 10.1088/1748-0221/15/03/C03014*.

[27] G. Baccani et al., The MIMA project. Design, construction and performances of a compact hodoscope for muon radiography applications in the context of Archaeology and geophysical prospections, JINST **13** (2018) no. 11, P11001. *DOI: 10.1088/1748-0221/13/11/P11001 [arXiv:1806.11398 [physics.ins-det]].*

[28] École Polytechnique and CNRS/IN2P3, OMEGA - Centre de Microélectronique (website). https://portail.polytechnique.edu/omega Accessed January 10, 2022.

[29] Raspberry Pi Foundation, RaspberryPi (website). https://www.raspberrypi.com Accessed January 10, 2022.

[30] Teledyne LeCroy, Teledyne LeCroy (website). https://teledynelecroy.com Accessed January 10, 2022.

[31] L. Bonechi et al., The MURAVES project and other parallel activities on muon absorption radiography, EPJ Web Conf. **182** (2018), 02015. *DOI: 10.1051/epjconf/201818202015*.

[32] G. Baccani et al., Muon Radiography of Ancient Mines: The San Silvestro Archaeo-Mining Park (Campiglia Marittima, Tuscany), Universe **5** (2019) no. 1, 34. *DOI: 10.3390/universe5010034*.

[33] L. Bonechi et al., Multidisciplinary applications of muon radiography using the MIMA detector, JINST **15** (2020) no. 05, C05030. *DOI: 10.1088/1748-0221/15/05/C05030*.

[34] G. Saracino et al., Imaging of underground cavities with cosmic-ray muons from observations at Mt. Echia (Naples), Sci. Rep. **7** (2017), 1181. *DOI: 10.1038/s41598-017-01277-3*.

[35] G. Baccani et al., The reliability of muography applied in the detection of the animal burrows within River Levees validated by means of geophysical techniques, Journal of Applied Geophysics **191** (2021), 104376. *DOI: 10.1016/j.jappgeo.2021.104376*.

[36] D. E. Groom et al., Muon stopping power and range tables 10-MeV to 100-TeV, Atom. Data Nucl. Data Tabl. **78** (2001), 183–356. *DOI: 10.1006/adnd.2001.0861*.

[37] L. Bonechi et al., Development of the ADAMO detector: test with cosmic rays at different zenith angles, 29th International Cosmic Ray Conference (Pune) **9** (2005) 283–286.

[38] J. Allison et al., Recent developments in Geant4, Nucl. Instrum. Meth. A **835** (2016), 186–225. *DOI: 10.1016/j.nima.2016.06.125*.

[39] D. Pagano et al., EcoMug: An Efficient COsmic MUon Generator for cosmic-ray muon applications, Nucl. Instrum. Meth. A **1014** (2021), 165732. *DOI: 10.1016/j.nima.2021.165732*.